Acta Crystallographica Section F
Structural Biology and Crystallization Communications
ISSN 1744-3091

Crystallization and preliminary crystallographic analysis of the *Clostridium perfringens* enterotoxin

David C. Briggs,[a]‡ James G. Smedley III,[b] Bruce A. McClane[b] and Ajit K. Basak[a]*

[a]Birkbeck College, University of London, England, and [b]Department of Microbiology and Molecular Genetics, University of Pittsburgh School of Medicine, Pittsburgh, USA

‡ Current address: Wellcome Trust Centre for Cell-Matrix Research, University of Manchester, England.

Correspondence e-mail: a.basak@mail.cryst.bbk.ac.uk

Received 16 December 2009
Accepted 5 May 2010

Clostridium perfringens is a Gram-positive anaerobic species of bacterium that is notable for its ability to produce a plethora of toxins, including membrane-active toxins (α-toxins), pore-forming toxins (ε-toxins) and binary toxins (ι-toxins). Here, the crystallization of the full-length wild-type *C. perfringens* enterotoxin is reported, which is the causative agent of the second most prevalent food-borne illness in the United States and has been implicated in many other gastrointestinal pathologies. Several crystal forms were obtained. However, only two of these optimized crystal forms (I and II) were useable for X-ray diffraction data collection. The form I crystals diffracted to $d_{\rm min}$ = 2.7 Å and belonged to space group $C2$, while the form II crystals diffracted to $d_{\rm min}$ = 4 Å and belonged to space group $P2_13$.

1. Introduction

During bacterial infection, many protein toxins released by the bacteria have cytotoxic activity. This toxicity is often accomplished by disrupting protein synthesis or cytoskeletal structure or by compromising the integrity of the plasma membranes. In some cases, a toxin forms pores to deliver an enzymatic component into the cytoplasm (Tilley & Saibil, 2006).

Pore-forming toxins (PFTs) are classified according to their architecture; for example, they can form an α-helical channel or a β-barrel. PFTs are a group of cytotoxic proteins with divergent protein structures (Anderluh & Lakey, 2008) which have the same activity, *i.e.* excessive permeability of a cell membrane, that ultimately leads to cell death. The loss in membrane fidelity caused by PFTs leads to the uncontrolled efflux of essential cytoplasmic components, such as amino acids, nucleotides, cofactors *etc.*, combined with an equally uncontrolled influx of Ca^{2+} ions and water, which can lead to the activation of cell-death pathways and unsustainable cell swelling, which can cause cell lysis (Gonzalez *et al.*, 2008).

Clostridium perfringens (CP) is a Gram-positive anaerobic rod-shaped spore-forming bacillus which is ubiquitous in the environment and is a natural inhabitant of the gastrointestinal tract of humans and animals (Songer & Uzal, 2005). The bacterium CP is an aetiological agent that causes a wide variety of diseases in humans and domestic animals and has become a paradigm species because of its environmental ubiquity, fast growth rate and oxygen tolerance and its ability to produce a range of extracellular protein toxins, *e.g.* α-toxin, β-toxin, ε-toxin, ι-toxin, enterotoxin (CPE) and several others. Some of these toxins are lethal and cause disease in humans and animals (Songer & Uzal, 2005; Brynestad & Granum, 2002). The ability of different strains of CP to cause disease has been ascribed mainly to differential production of these exotoxins (McClane *et al.*, 2006). However, individual isolates produce a specific subset of these toxins and based on the production of α-, β-, ε- and ι-toxins the bacterium CP can be classified into five different serotypes (A–E).

The enterotoxin (CPE) is the virulence determinant of type A food poisoning and other gastrointestinal (GI) diseases (McClane & Chakrabarti, 2004). CPE is produced by type A strains and these strains also cause hospital-acquired and community-acquired anti-

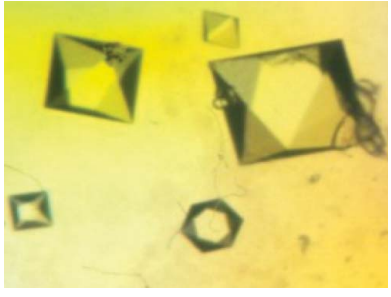

biotic associated diarrhoea (AAD) and sporadic diarrhoea (SD), which are more severe than normal type A food-borne diseases. CPE has also been linked to some veterinary GI diseases (Meer *et al.*, 1997).

CPE (UniProt P01558) is a single polypeptide chain consisting of 319 amino acids and with a molecular mass of ∼35 kDa. This protein is produced in large amounts by *C. perfringens* during sporulation (∼15% of dry cell mass). In common with other PFTs, it is synthesized as a less active pre-protein and is probably activated upon release into the host gut by endogenous proteases such as trypsin and chymotrypsin (Granum, 1986). One difference between CPE and other PFTs is that CPE is not actively secreted; rather, it is released upon cell lysis when the spore is released. After release and proteolytic activation in the mammalian gut, CPE associates with its receptor(s), which include members of the claudin family of transmembrane proteins that are found in tight junctions (McClane, 2001).

Whilst some molecular events leading to CPE pore formation are presently unclear, SDS-resistant CPE-containing complexes have been isolated with masses of 425–500 and 550–660 kDa and are thought to consist of a CPE hexamer and differing amounts of various CPE-receptor claudins, nonreceptor claudins and (for the 550–660 kDa complex) occludin (Robertson *et al.*, 2007). Claudins and occludin are found in tight junctions between cells in gut epithelia and are involved in maintaining the integrity of the tight junction (Hossain & Hirata, 2008). In addition to this, they also act as functional receptors for CPE, allowing toxin concentrations to be maximized at the cell membrane. This in turn facilitates CPE pore formation.

CPE also contains a sequence pattern containing alternating hydrophobic and hydrophilic amino-acid residues (residues 81–106) that is characteristic of amphipathic β-strands seen in β-pore-forming toxins, and pre-pore complexes have also been identified biochemically (Smedley *et al.*, 2007). Because of these observations, CPE is presumed to be a novel variant of the β-pore-forming toxins. The structure of the claudin-binding domain (residues 197–319) has recently been solved (Van Itallie *et al.*, 2008); however, since the N-terminal CPE sequences are required for oligomerization and pore formation (Kokai-Kun & McClane, 1996; Smedley *et al.*, 2007), it is important to solve the structure of the native CPE protein in order to fully understand this toxin's action.

Over the last few decades, CPE has been the subject of intense research; however, how the CPE protein mediates its action during disease is not yet fully understood at the molecular level. Here, we report the crystallization and preliminary X-ray diffraction data characterization of CPE.

2. Materials and methods

2.1. Protein isolation, purification and concentration

Protein was isolated from sporulating *C. perfringens* strain NCTC 8239 as described by McDonel & McClane (1988). Briefly, wild-type CPE (UniProt P01558, 319 residues, molecular weight 33 530) was harvested from *C. perfringens* NCTC 8239 that had been induced to sporulate in Duncan–Strong medium. Monodisperse protein of high purity was obtained by sequential ammonium sulfate precipitation steps followed by size-exclusion chromatography. The final purified CPE preparation appeared as a single band upon native electrophoresis. This purified CPE was shipped from the USA to the UK under export license D388080 from the United States Department of Commerce, Bureau of Industry and Security.

Owing to the instability of the CPE protein at ambient temperature, all crystallization screening and crystal manipulation was carried out at 277 K. Attempts to concentrate the protein using standard methods (using either nitrogen stirred cells or centrifugal concentrators) were unsuccessful and we postulate that this may arise from the hydrophobic membrane-interacting surface patches that are likely to be present within the protein irreversibly binding to the membrane used in these concentration techniques. Using these techniques, we were unable to obtain protein concentrations in excess of 5 mg ml^{-1} and concentration to this level resulted in the loss of more than 60% of the protein.

In order to overcome this problem, we devised an alternative concentration technique. The protein preparations were desalted using G25 resin contained in a PD-10 gravity-flow column. Protein was eluted using Milli-Q water. Following this, the protein was placed

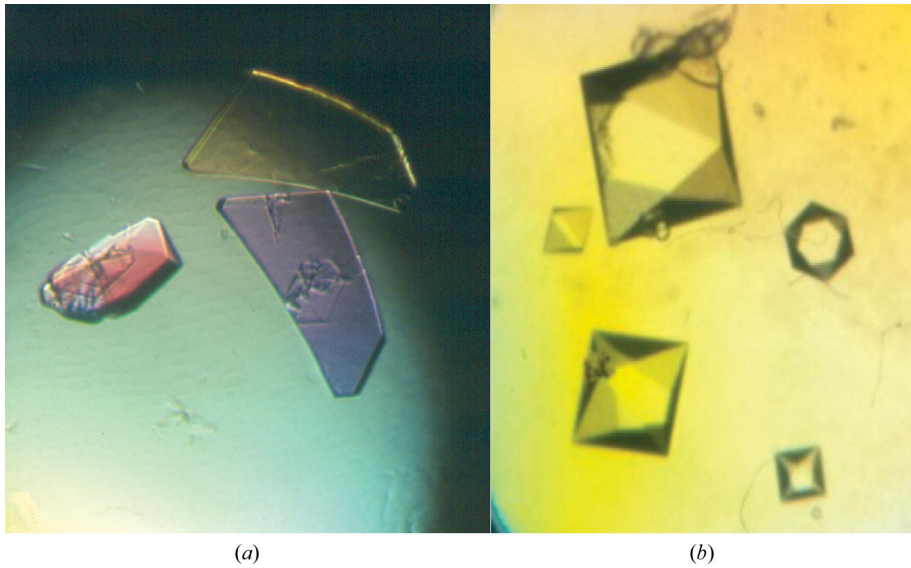

(*a*) (*b*)

Figure 1
(*a*) Crystals of form I; the cracking visible on the crystals is a consequence of the change in temperature on moving the crystals from 277 K to ambient temperature. Crystal dimensions are approximately 200 × 100 × 20 µm. (*b*) Crystals of form II. The largest crystal has dimensions of approximately 400 × 300 × 300 µm.

in a 1.5 ml capacity Eppendorf tube modified with an ∼2 mm diameter hole punched in the lid. This Eppendorf tube was then spun in a Howe Gyrovap at 10 000*g* in a partial vacuum (∼200 Pa). Using this 'incomplete desiccation' technique, the water within the sample was slowly removed and the protein could be concentrated to 30 mg ml^{-1} without any precipitation. Throughout this procedure, protein loss did not exceed 10% of the starting amount.

Electrospray mass spectrometry (ESI–MS) of the sample following this process revealed a single species of mass 33 539 ± 15 Da, which is consistent with the theoretical mass of the intact protein (33 530 Da); circular-dichroism spectroscopy gave a spectrum characteristic of an all-β-sheet protein (data not shown), which is in agreement with previously published data (Granum, 1986). These data indicate that CPE is not damaged or denatured by this concentration technique.

2.2. Crystallization

Initial crystallization conditions were screened by the sitting-drop vapour-diffusion and microbatch techniques at 277 K using commercially available screening solutions including Crystal Screen, Crystal Screen 2 and Crystal Screen Lite (Hampton Research). A number of conditions produced initial crystals and attempts were made to optimize the crystal quality. However, only two of these optimized conditions produced better quality crystals (forms I and II) that were suitable for X-ray diffraction studies.

2.2.1. Crystal form I. Crystal form I was grown by the sitting-drop vapour-diffusion technique using dioxane as a precipitant. Each drop contained 1 µl protein solution at 14 mg ml^{-1} in Milli-Q water containing 0.1%(*w*/*v*) β-octyl glucoside (added to the protein drop only) mixed with an equal volume of reservoir solution and was equilibrated at 277 K against 500 µl reservoir solution composed of 32–40%(*v*/*v*) dioxane in water. Crystals appeared after one week and had an irregular plate-like appearance (Fig. 1*a*). The crystals were cryoprotected in crystallization buffer supplemented with 28%(*v*/*v*) glycerol and vitrified in liquid nitrogen. Diffraction data were collected to a resolution of 2.7 Å on station ID14-EH4 at the ESRF.

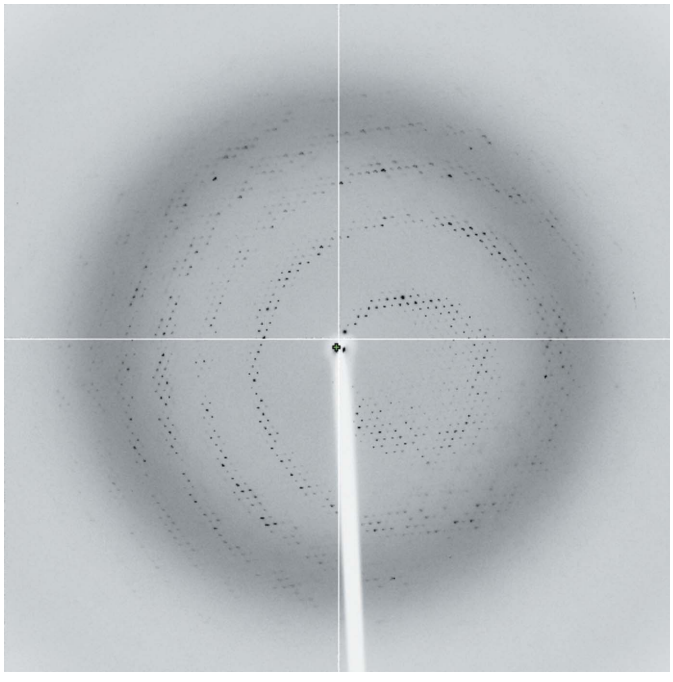

Figure 2
Typical diffraction from a form I crystal.

Table 1
Data-processing statistics.

	Form I	Form II
No. of crystals	1	1
Beamline	ID14-EH4	ID14-EH4
Wavelength (Å)	0.9686	1.2823
Detector	ADSC	ADSC
Crystal-to-detector distance (mm)	260	300
Rotation range per image (°)	1.0	0.5
Total rotation range (°)	200–360	200–300
Exposure time per image (s)	1	1
Resolution range (Å)	70.0–2.68 (2.82–2.68)	70.0–4.2 (4.5–4.2)
Space group	*C*2	$P2_13$
Unit-cell parameters (Å, °)	a = 211.1, b = 119.5, c = 74.7, β = 110.6	$a = b = c$ = 159.7
Mosaicity (°)	0.70	0.74
Total No. of measured intensities	95985 (13648)	117517 (12401)
Unique reflections	42488 (6259)	11727 (1667)
Multiplicity	2.7 (2.4)	10.4 (10.0)
Mean $I/\sigma(I)$	12.0 (2.2)	16.7 (6.6)
Completeness (%)	95.8 (83.3)	99.9 (100.0)
$R_{\rm merge}$† (%)	0.089 (0.361)	0.157 (0.395)
$R_{\rm p.i.m.}$‡ (%)	0.056 (0.272)	0.065 (0.259)
Overall B factor from Wilson plot (Å^2)	70.8	79.1

† $R_{\rm merge} = \sum_{hkl}\sum_i |I_i(hkl) - \langle I(hkl)\rangle| / \sum_{hkl}\sum_i I_i(hkl)$. ‡ $R_{\rm p.i.m.} = \sum_{hkl}[1/(N-1)]^{1/2} \times \sum_i |I_i(hkl) - \langle I(hkl)\rangle| / \sum_{hkl}\sum_i I_i(hkl)$, where N is the data redundancy, $I_i(hkl)$ is the observed intensity and $\langle I(hkl)\rangle$ is the mean intensity of multiple observations of symmetry-related reflections.

Typical diffraction from these crystals is shown in Fig. 2. Analysis of the data indicated that the crystals belonged to space group *C*2, with unit-cell parameters a = 211.1, b = 119.5, c = 74.7 Å, β = 110.6°.

The Matthews coefficient indicated that the asymmetric unit contained between three and six monomers ($V_{\rm M}$ = 4.20 Å^3 Da^{-1} for three molecules in the asymmetric unit with an estimated solvent content of 71%; $V_{\rm M}$ = 2.10 Å^3 Da^{-1} for six molecules in the asymmetric unit with 41% solvent content). Data statistics are given in Table 1. Self-rotation function calculations carried out with the program *POLARRFN* (Collaborative Computational Project, Number 4, 1994), using all data and Patterson radii between 20 and 40 Å with a sharpening of −30 to −100 Å^2 applied, consistently gave a distinctive non-space-group symmetry-related peak in the κ = 120°

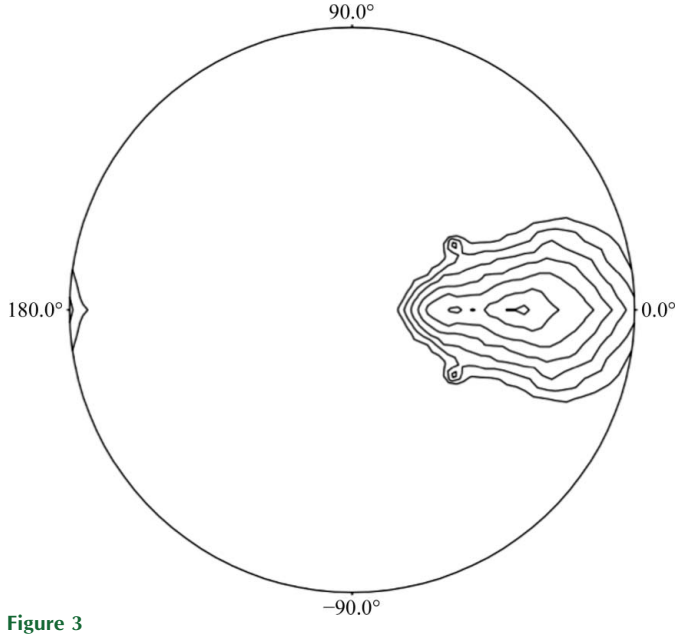

Figure 3
Stereographic projection of the κ = 120° section of the self-rotation function from crystal form I native data. The polar angles defining the NCS threefold are ω = 68.6°, φ = 0°.

section with polar angles $\omega = 68.6^\circ$ and $\varphi = 0^\circ$, indicating the presence of noncrystallographic threefold symmetry; however, no clear peaks were observed at $\kappa = 60^\circ$ to support sixfold noncrystallographic symmetry. Fig. 3 provides an example of the $\kappa = 120^\circ$ section, with a Patterson radius of 25 Å and -100 Å^2 sharpening.

2.2.2. Crystal form II. Crystal form II was obtained using the microbatch technique. 1 µl of 10 mg ml^{-1} protein solution (in Milli-Q water) was mixed with an equal volume of crystallization buffer composed of 50 m*M* citrate buffer pH 4.3, 10 m*M* $ZnCl_2$ and 1.4 *M* hexane-1,6-diol and incubated under 4 ml paraffin oil using Terasaki microbatch plates. Crystals appeared after 16 weeks and had tetragonal bipyramidal morphology (Fig. 1*b*). The crystals were cryoprotected in a solution consisting of 50 m*M* citrate buffer pH 4.3, 10 m*M* $ZnCl_2$ and 2 *M* hexane-1,6-diol and were vitrified in liquid nitrogen. Diffraction data were collected at station ID14-EH4 at the ESRF to a resolution of 4.2 Å. Indexing of the data suggested that the crystals were of primitive cubic lattice type, with unit-cell parameters $a = b = c = 159.7$ Å.

Analysis of the self-rotation function suggested that the data belonged to Laue class *m*3*m*; however, cumulative intensity distributions suggested that this crystal form suffers from merohedral twinning and that the true Laue class is 3*m*, with the only possible twinning operator being $k, h, -l$. Analysis of statistics provided by the *DETWIN* program (Yeates, 1997) indicated a twin fraction of 0.45.

The Matthews coefficient indicated that for Laue class 3*m* the asymmetric unit contains between two ($V_M = 4.85$ Å^3 Da^{-1}, estimated solvent content 75%) and four ($V_M = 2.4$ Å^3 Da^{-1}, estimated solvent content 49%) monomers. No significant noncrystallographic peaks were seen in the self-rotation function at $\kappa = 180^\circ$ or 90°.

2.3. Data processing

Data sets for both crystal forms were processed with the *MOSFLM* program (Leslie, 1992). Scaling and merging of the data were performed using the program *SCALA* (Evans, 1993). All subsequent data manipulations were carried out with *CCP*4 software (Collaborative Computational Project, Number 4, 1994).

Data statistics for both crystal forms I and II are listed in Table 1.

2.4. Phasing

Our attempt to determine the phases of CPE using the coordinates of the recently determined three-dimensional structure of the carboxyl-terminal domain of CPE (residues 197–319; PDB code 2quo; Van Itallie *et al.*, 2008), which has also been identified as the claudin-binding domain, was not successful. We anticipate that combining phase information from other sources, for example heavy-atom derivative data, with phasing using 2quo will be necessary to resolve the three-dimensional structure of the whole CPE molecule.

The authors wish to thank Dr Robert Sarra for his assistance with ESI–MS and CD spectroscopy and the beamline staff at ID14-EH4, ESRF, Grenoble, France for assistance with data collection.

References

Anderluh, G. & Lakey, J. H. (2008). *Trends Biochem. Sci.* **33**, 482–490.
Brynestad, S. & Granum, P. E. (2002). *Int. J. Food Microbiol.* **74**, 195–202.
Collaborative Computational Project, Number 4 (1994). *Acta Cryst.* D**50**, 760–763.
Evans, P. R. (1993). *Proceedings of the CCP4 Study Weekend. Data Collection and Processing*, edited by L. Sawyer, N. Isaacs & S. Bailey, pp. 114–122. Warrington: Daresbury Laboratory.
Gonzalez, M. R., Bischoffberger, M., Pernot, L., van der Goot, F. G. & Freche, B. (2008). *Cell. Mol. Life Sci.* **65**, 493–507.
Granum, P. E. (1986). *Proceedings of the Second European Workshop on Bacterial Protein Toxins*, edited by P. Falmagne, J. Alouf, F. Fehrenbach, J. Jeljaszewicz & M. Thelestam, pp. 327–334. Stuttgart: Gustav Fischer.
Hossain, Z. & Hirata, T. (2008). *Mol. Biosyst.* **12**, 1181–1185.
Kokai-Kun, J. & McClane, B. (1996). *Infect. Immun.* **64**, 1020–1025.
Leslie, A. G. W. (1992). *Jnt CCP4/ESF–EACBM Newsl. Protein Crystallogr.* **26**.
McClane, B. A. (2001). *Toxicon*, **39**, 1781–1791.
McClane, B. A. & Chakrabarti, G. (2004). *Anaerobe*, **10**, 107–114.
McClane, B. A., Uzal, F. A., Fernandex-Miyakawa, M. E., Lyerly, D. & Wilkins, T. (2006). *The Prokaryotes: A Handbook on the Biology of Bacteria*, edited by M. Dworkin, Vol. 4, ch. 1.2.22. New York: Springer.
McDonel, J. L. & McClane, B. A. (1988). *Methods Enzymol.* **165**, 94–103.
Meer, R. R., Songer, J. G. & Murrell, W. G. (1997). *Rev. Environ. Contam. Toxicol.* **150**, 75–94.
Robertson, S. L., Smedley, J. G. III, Singh, U., Chakrabarti, G., Van Itallie, C. M., Anderson, J. M. & McClane, B. A. (2007). *Cell. Microbiol.* **9**, 2734–2755.
Smedley, J. G. III, Uzal, F. A. & McClane, B. A. (2007). *Infect. Immun.* **75**, 2381–2390.
Songer, J. G. & Uzal, F. A. (2005). *J. Vet. Diagn. Invest.* **6**, 528–536.
Tilley, S. J. & Saibil, H. R. (2006). *Curr. Opin. Struct. Biol.* **16**, 230–236.
Van Itallie, C. M., Betts, L., Smedley, J. G. III, McClane, B. A. & Anderson, J. M. (2008). *J. Biol. Chem.* **283**, 268–274.
Yeates, T. O. (1997). *Methods Enzymol.* **276**, 344–358.